Nuclear Materials Authority
P.O. Box 530, El Maddi, Cairo, Egypt

ISSN 2314-5609
Nuclear Sciences Scientific Journal
13, 100-109
2024
https://nssi.journals.ekb.eg

SYNTHESIS AND CHARACTERIZATION OF HEMATITE NANOPARTICLES FOR REMOVAL OF PB^{2+} AND CU^{2+}FROM WATER SAMPLES

MOHAMED MOHAMED GOUDA

Geology of Isotopes, Nuclear Materials Authority, El Maadi, Cairo, Egypt

ABSTRACT

Heavy metal ions in water samples have potential hazard to human health. So, treatment of waste water is a necessity to decrease the levels of such hazard metals. The present study described a method for wastewater samples treatment using magnetic nanoparticles. Hematite nanoparticles (αFe_2O_3NPs) were synthesized and characterized using transmission electron microscope (TEM) and X-ray diffraction (XRD). The prepared αFe_2O_3NPs were used for solid phase adsorption of Pb^{2+} and $Cu^{2+}$from aqueous solutions. The effects of various parameters, including solution pH, shaking time, and adsorbent dose on adsorption efficiency were investigated. Langmuir adsorption isotherm was effectively described the adsorption process onto αFe_2O_3NPs. The study found that Pb^{2+} and Cu^{2+}adsorption was quantitative at pH 5.5, with maximum adsorption capacities of 200 mg g^{-1} and 15.3 mg g^{-1} for Pb^{2+} and Cu^{2+}, respectively, under optimum conditions. This method was found to be applicable for the removal of Pb^{2+} and $Cu^{2+}$from water samples.

Keywords: αFe_2O_3; nanoparticles; adsorption, metal ions; solid phase extraction

INTRODUCTION

Heavy metal ions are widespread environmental pollutants, and the presence of these elements including Pb^{2+} and Cu^{2+}in river water is a major concern due to their potential harm to public health, living organisms, and freshwater supply [1,2]. These non-biodegradable metal ions can cause kidney damage, nervous system damage, and renal dysfunction when exposure exceeds safe levels [3,4]. As a result, regulations to reduce heavy metal ions concentration in water are becoming increasingly stringent to mitigate these harmful effects [5]. While the simultaneous removal of multiple hazardous heavy metal ions offers a cost-effective solution, it has been challenging to achieve due to the competing adsorption of these heavy metal ions. Nevertheless, it is crucial to develop an effective and low-cost strategy to avoid the repeated one-by-one removal of pollutants.

Solid phase extraction (SPE) is a highly effective and affordable method for recovery or removal of substances, and its versatility has made it widely used [4]. The success of SPE relies heavily on the sorbent used, and the search for new sorbents with high surface area, fast sorption kinetics, and stability over a wide pH range has become increasingly important. However, traditional sorbents such as clay minerals and oxides have limited sorption capacity and efficiency. Recent studies have shown that nanomaterials, such as nano-oxides, nanocarbon, and carbon-based nanocomposites [5–9], exhibit exceptional sorption capacity. Despite their potential, the high dispersibility of nanomaterials in aqueous solutions has made it difficult to separate the sorbents from the aqueous phase once saturation is reached, limiting their application in large volumes of water.

In recent times, there has been an increasing interest in magnetic nanoparticles (MNPs), particularly iron oxide due to their remarkable characteristics such as low toxicity and ease of separation [10-13]. By placing a magnet outside the extraction container, MNPs can be readily separated from the sample solution. Consequently, magnetic solid phase extraction (MSPE) is advantageous because of its speed, affordability, simplicity, and reusability.

In this work, αFe_2O_3 NPs as low-cost abundant material was synthesized in nano form and characterized using XRD and TEM. The prepared nano magnetite was used for Pb^{2+} and Cu^{2+}removal from aqueous solution. The effect of different factors on the adsorption was investigated and optimized. The nano magnetic material was used to adsorb metal ions from real sample solution.

EXPERIMENTAL

Reagents

All chemicals and reagents were of analytical grade. Every day, a working standard solution of Pb^{2+} and $Cu^{2+}$was prepared by progressively diluting a standard stock solution of 1000 mg L^{-1}, obtained from Merck (Darmstadt, Germany), in ultra-pure water.

Synthesis of Fe_3O_4 nanoparticles

The conventional co-precipitation method was used with slight modifications [14, 15] to synthesize αFe_2O_3nanoparticles. A mixture of 11.68 g of ferric chloride and 4.30 g of ferrous chloride was dissolved in 200 mL of high-purity water under nitrogen gas with vigorous stirring at 85°C. Then, 40 mL of 30% (v/v) NH_3. Then H_2O was added with increased nitrogen passing rate and stirring speeds, resulting in an immediate color change from orange-red to black. After half an hour, the reaction was stopped, and the obtained suspension was left to cool naturally to room temperature. The nanoparticles were then washed repeatedly with high-purity water, 0.02 mol/L sodium chloride, and ethanol. Finally, the cleaned nanoparticles were stored in an ethanoate solution with a concentration of 40 g/L.

Apparatus

The JEOL 1011 microscope was utilized to perform transmission electron microscopy (TEM) characterization at 100 kV. A Fe_2O_3NPs suspension in ethanol was placed on a carbon-coated copper grid and dried under vacuum. X-ray diffraction was conducted using a PANalytical Empyrean diffractometer equipped with a cobalt source, a Bragg-Brentano HD optics, and a PIXcel1D-Medpix3 detector with specified parameters. Measurement of the pH of the test solutions was performed using pH meter electrodes (Horiba F-22). To determine the concentration of heavy metal ions, a Thermo Electron Corporation-S series Atomic Absorption Spectrometer was utilized. The spectrometer was equipped with a deuterium lamp for background correction, the manufacturer's recommended operating conditions were followed, unless otherwise specified.

Experimental uptake of heavy metal ions

The adsorption experiments for heavy metal ions uptake were conducted using the batch technique in a series of flasks. In each flask, 10mg of αFe_2O_3NPs was added to 20 mL of Cu^{2+} and Pb^{2+}solution. The flasks were agitated on a Vibromatic-384 shaker at 120 rpm for 15 minutes at room temperature. The pH of the solution was measured using a Corning 125 pH-meter. The residual concentration of heavy metal ions at equilibrium was analyzed using Flame Atomic Absorption spectrometry.

The removal Percentage (R) and the adsorption capacity for $Pb^{2+}$and Cu^{2+}were calculated according to Eq.1 and Eq. 2, respectively.

$$R = \frac{C_0 - C_e}{C_0} \times 100\% \quad (1)$$

$$Q_e = \frac{(C_0 - C_e)V}{W} \quad (2)$$

where Q_e is the adsorption capacity (mgg^{-1}). C_o, C_e is the initial and equilibrium $Pb^{2+}$and Cu^{2+}concentrations in the aqueous phase (mgL^{-1}), respectively, V is the volume of heavy metal ions solution, (L) and W is the weight of dry αFe_2O_3 NPs(g).

RESULTS AND DISCUSSION

Characterization of αFe_2O_3 nanoparticles

Fig. 1 displays the X-ray diffractogram of the produced α Fe_2O_3 nanoparticles. The diffractogram reveals that only six characteristic peaks of hematite αFe_2O_3, specifically (2θ = 21.1°, 35.1°, 41.4°, 50.5°, 63° and 67.4°) with Miller indices (012), (110),(113), (024), (214) and (441), respectively, were identified in both samples (a and b).

TEM was used to determine the morphology and size of the prepared NPs. TEM micrographs of α Fe_2O_3 at different magnification were presented in Fig.2a, b,c. The nanoparticles are spherical and polydisperse with an average size of 11 nm as observed by TEM and the corresponding size distribution histograms of these NPs (Fig. 2d).

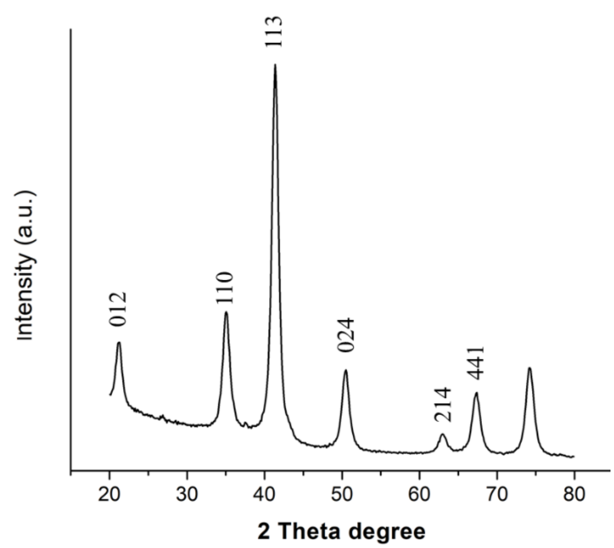

Fig. 1. XRD patterns of the synthesized αFe_2O_3 nanoparticles.

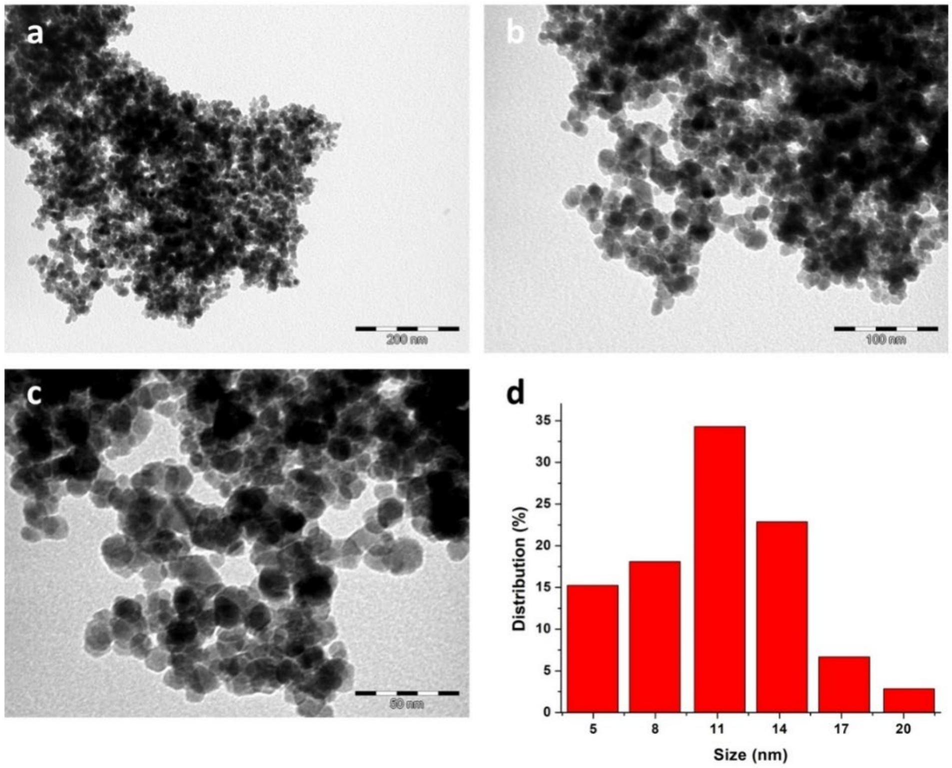

Fig. 2. Transmission electron micrographs of αFe_2O_3 nanoparticles at different magnification. a) 200 nm b)100 nm C)50 nm. D) Corresponding particle size distribution histograms of the synthesized αFe_2O_3 NPs.

Optimization of adsorption of metal ions onto αFe_2O_3 nanoparticles

Effect of pH

The pH value of the aqueous solution plays a crucial role in controlling the adsorption process of metal ions at the solid-liquid interface. To investigate the effect of pH on Pb^{2+} and Cu^{2+}adsorption onto αFe_2O_3 nanoparticles, experiments were carried out at different pH levels ranging from 1 to 8 while maintaining other experimental parameters constant. The results, presented in Fig.3, demonstrate that the adsorption efficiency increases with an increase in pH reaching maximum at pH 5.5 for both Pb^{+2} and Cu^{+2}. It is possible that the reason for the lower adsorption efficiency of metal ions at lower pH is due to the higher proton (H^+) density in the medium. This can lead to competition between H^+ and metal ions for active sites on the αFe_2O_3 nanoadsorbents, resulting in fewer active adsorption sites being available for metal ions [16].Another reason was attributed to the surface charge of the αFe_2O_3nanoadsorbents, as magnetite nanoparticles have amphoteric surface activity [17]. In water-based environments, the surface of magnetite nanoparticles is covered with FeOH. This layer can either gain or lose protons depending on the pH of the medium, resulting in the formation of FeO^- or $Fe(OH)^{2+}$ species.

Effect of contact time

The impact of shaking time on the adsorption of Pb^{2+} and Cu^{2+}at an initial concentration of 20 mg L^{-1} using 20 mg of αFe_2O_3 NPs was examined by varying the shaking time between 3 and 30 minutes, as shown in Figure 4. The findings revealed that the highest adsorption efficiency of Pb^{2+} and Cu^{2+} was achieved after 15 minutes of shaking.

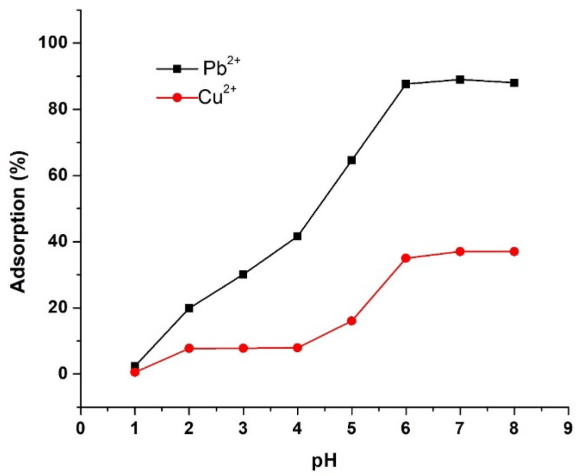

Fig. 3. Effect of pH on adsorption efficiency of Pb^{2+} and Cu^{2+}on αFe_2O_3 nanoparticles. Conditions: αFe_2O_3 nanoparticles (20 mg), Pb^{2+}(20 mg L^{-1}), Cu^{2+} (20 mg L^{-1}), V (20 mL) at room temperature.

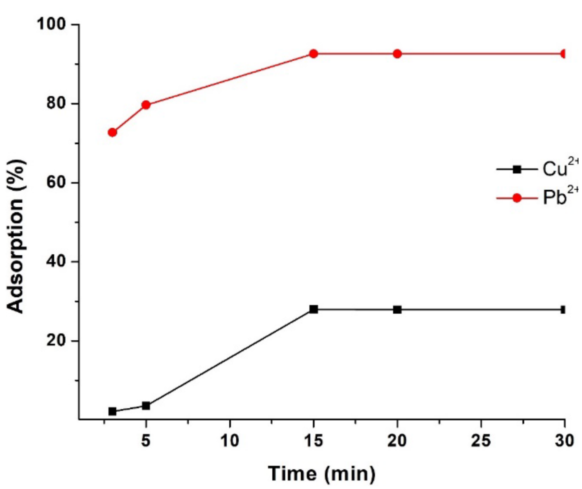

Fig. 4. Effect of shaking time on the adsorption efficiency of Pb^{2+} and Cu^{2+}. Conditions: αFe_2O_3 NPs (20 mg), Pb^{2+}(20 mg L^{-1}), Cu^{2+}(20 mg L^{-1}),V (20 mL) at room temperature.

Effect of adsorbent amount

The experiments were conducted using different amounts of adsorbent ranging from 5 to 20 mg, with an initial concentration of 10 mg $L^{-1}$for both Pb^{2+} and Cu^{2+}, in 20 mL of solution at a temperature of 25°C and pH of 5.5. The results, shown in Figure 5, indicate that the adsorption efficiency of Pb^{2+} and Cu^{2+} increased with the dosage of αFe_2O_3 up to 15 mg, reaching maximum of 87% and 60% for Pb^{2+} and Cu^{2+}, respectively. Further increase in the adsorbent dosage did not result in significant improvement in adsorption efficiency, followed by a plateau.

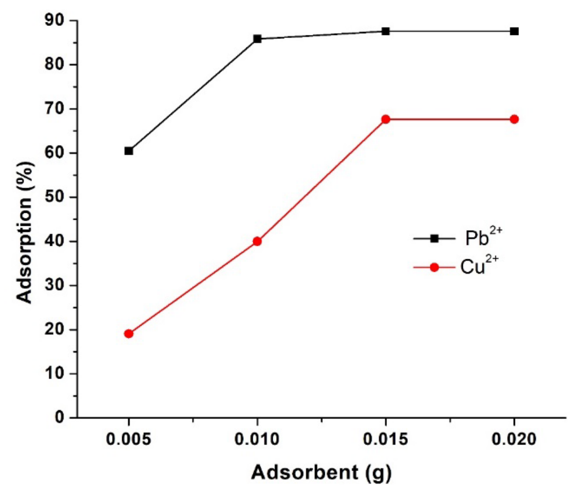

Fig. 5. Effect of αFe_2O_3 NPs amount on the adsorption efficiency of Pb^{2+} and Cu^{2+}. Conditions: Pb^{2+} (10 mg L^{-1}), Cu^{2+} (10 mg L^{-1}), pH (5.5), shaking time (15 min), (20 mL) at room temperature.

Adsorption isotherms

Freundlich and Langmuir models were used to discuss the adsorption isotherm of Pb^{2+} and Cu^{2+} on αFe_2O_3 NPs.

Freundlich isotherm model was employed to describe an empirical relation between the concentration of Pb^{2+} and Cu^{2+}adsorbed on the surface of αFe_2O_3 NPs and the concentration of the metal ions in the solution, which characterizes a heterogeneous adsorption system. The linear form of the Freundlich model is shown in Equation (3) [19],

$$lnQ_e = lnK_f + \frac{ln\,C_e}{n} \quad (3)$$

where Q_e is the equilibrium adsorption capacity (mgg^{-1}), C_e is the equilibrium concentration of Pb^{2+} and Cu^{2+}in solution(mgL^{-1}), K_f and 1/n are Freundlich constants.

A Freundlich plot of lnQ_e versus lnC_e would result in a straight line with a slope of 1/n and an intercept of lnK_f, as shown in Fig. 6b and Fig. 6d for Pb^{2+} and Cu^{2+}, respectively. The values of 1/n indicate whether the nature of the isotherm is unfavorable (1/n > 1), favorable (0 < 1/n < 1), or irreversible (1/n = 0). In this study, the values of 1/n were found between 0 and 1 (Table 1), which means that the adsorption of Pb^{2+} and Cu^{2+} onto αFe_2O_3 NPs is favorable.

Langmuir isotherm: The linear form of the Langmuir model is expressed in Equation (4) [20],

$$\frac{C_e}{Q_e} = \frac{1}{bQ_{max}} + \frac{C_e}{Q_{max}} \quad (4)$$

where C_e is the equilibrium concentration of the metal ions in the solution, Q_e is the adsorption capacity at equilibrium, Q_{max} is the maximum adsorption capacity, and b is the binding constant. A straight line is obtained by plotting C_e/Q_e versus C_e, as shown in Fig. 6a and Fig. 6c for Pb^{2+} and Cu^{2+}, respectively. The Langmuir parameters can be used to predict the affinity between the sorbate and sorbent. According to the Langmuir isotherm model, the adsorption process is uniform on the surface of adsorbent and once the active sites occupied by the sorbate, no more sorption occurs at these sites.

The Langmuir adsorption isotherm can be represented using a dimensionless constant called the equilibrium parameter R_L, which is defined Equation (5):

$$R_L = \frac{1}{1+bC_o} \quad (5)$$

The R_L value is an indicator of the nature of the isotherm, which can be unfavorable (R_L> 1), linear (R_L = 1), favorable (0 < R_L< 1), or irreversible (R_L = 0) [21,22]. Fig.7 shows the plot of R_L vs. C_o, for both Pb^{2+} and Cu^{2+}.The calculated R_L values ranged between 0 and 1 for Pb^{2+} (Fig. 7a). This suggests that the adsorption of Pb^{2+} onto αFe_2O_3 NPs is favorable under the conditions used in this study. As the initial concentration of Pb^{2+}increased, the R_L values decreased, indicating that the adsorption of metal ions is more effective at higher initial concentrations.

On the otherside, the R_L of $Cu^{2+}$is more than 1 for Cu^{2+}(Fig. 7b). The R_L values increased as Cu^{2+} initial concentration increased. It suggests that the adsorption of Cu ions onto αFe_2O_3 NPs is unfavorable. This finding explains the lower adsorption capacity of Cu^{2+} onto αFe_2O_3 NPs

The results of Adsorption isotherms models indicated that the adsorption of both Pb^{2+} and Cu^{2+} onto αFe_2O_3 NPs was well-fitted with the Langmuir model (R^2 = 0.99), which is closer to unity than the Freundlich model. The Langmuir and Freundlich constants for Pb^{2+} and Cu^{2+} are summarized in Table 1.

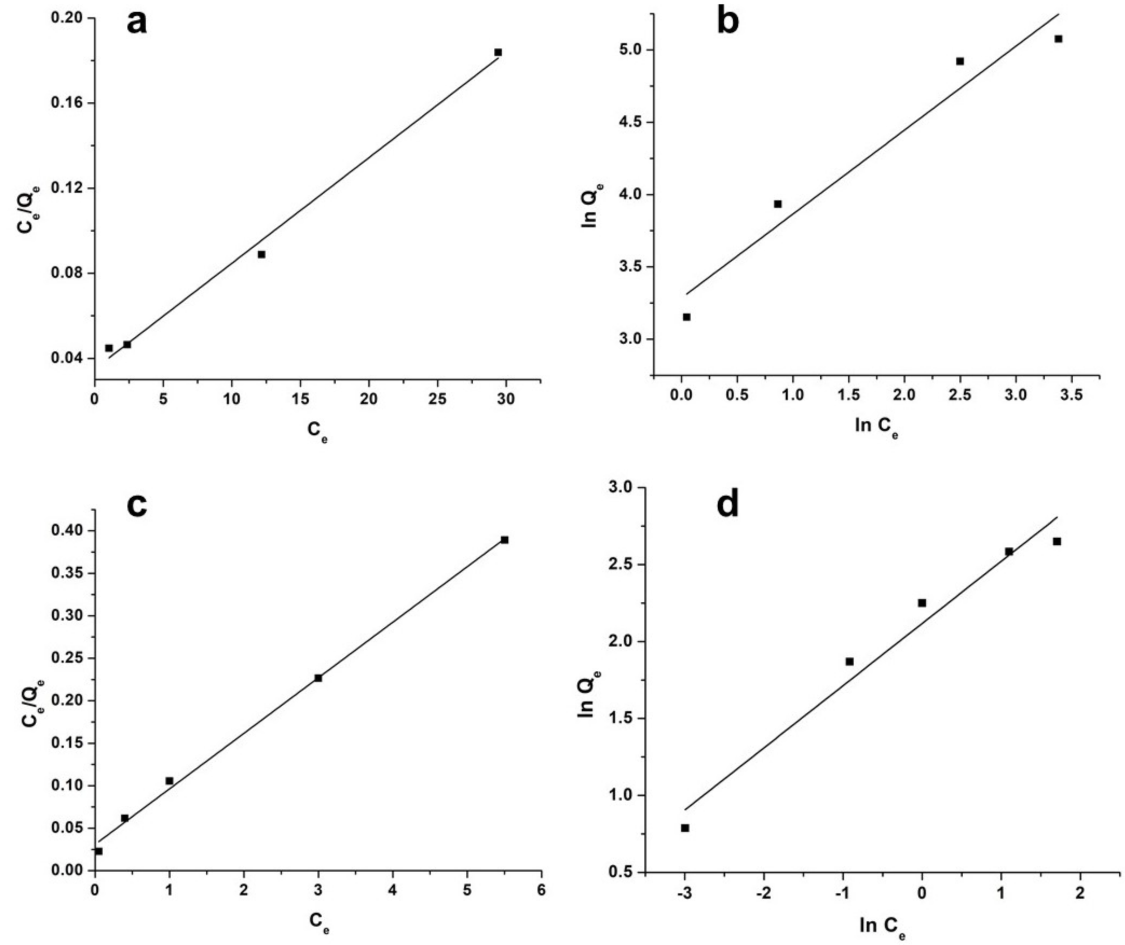

Fig. 6. Adsorption isotherms of Pb^{+2} and Cu^{+2} onto hematite NPs. (a) Langmuir isotherm of Pb^{+2}. (b) Freundlich isotherm of Pb^{+2}. (c) Langmuir isotherm of Cu^{+2}. (d) Freundlich isotherm of Cu^{+2}.

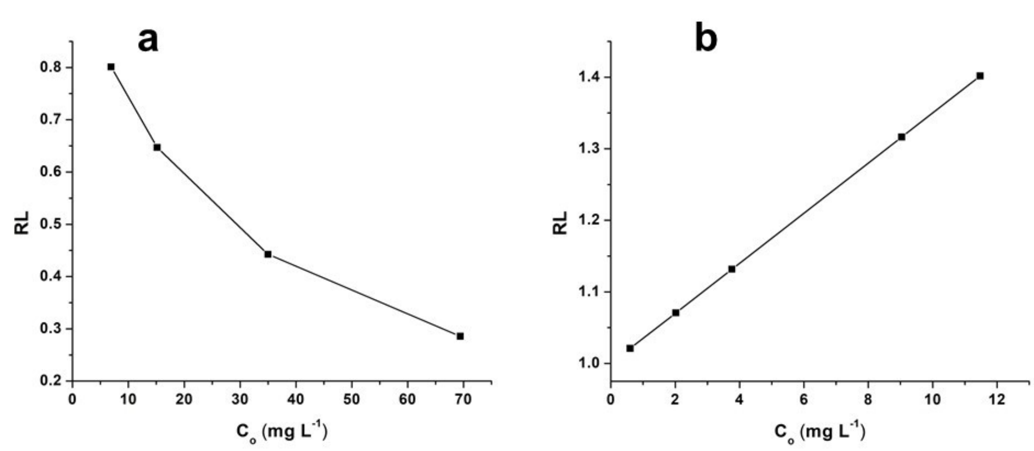

Fig. 7. Variation of adsorption intensity (R_L) with initial concentration (C_o). (a) Pb^{2+} and (b) Cu^{2+}.

Table 1. Langmuir and Freundlich parameters for Pb^{2+} and Cu^{2+} adsorption onto αFe_2O_3 NPs.

Metal ions	Linear Langmuir model parameters			Freundlich model parameters		
	Q_{max}(mg g^{-1})	b(L mg^{-1})	R^2	K_f	$1/n$	R^2
Pb^{2+}	15.3	0.036	0.99	8.3	0.4	0.96
Cu^{2+}	200	0.035	0.99	26.7	0.58	0.95

Application

The αFe_2O_3 NPs were utilized for the removal of Pb^{2+} and Cu^{2+}ions from spiked real water samples including tab water and wastewater. The wastewater sample solution was collected from sewage. Table 2 summarize the chemical analysis of the major elements present in tap water and wastewater. Every water sample was spiked with different amount of $Pb^{2+}$and Cu^{2+}.A total solution of 20 mL of the waste sample with pH 5.5 was treated with appropriate amount of αFe_2O_3 NPs at room temperature for 15 min. The results showed that the αFe_2O_3 NPs successfully removed a high percentage of Pb^{2+} and Cu^{2+} from tap water and wastewater (Table 3).

Table 2. Chemical analysis of major elements in water samples.

	Na (ppm)	K (ppm)	Ca (ppm)	Mg (ppm)
Tap water	33.3	5.55	400.8	243.2
wastewater	4000	60	481	389.12

Table 3. Application of αFe_2O_3NPs for removal of different amounts of $Pb^{2+}$and Cu^{2+}in spiked water samples

	Pb			Cu		
	Added (ppm)	After (ppm)	Removal%	Added (ppm)	After (ppm)	Removal (%)
Tap water	2.05	0.12	94.1	2.49	0.19	92.4
	4.28	0.33	92.3	4.70	0.39	91.7
Wastewater	2.48	0.08	96.8	2.22	0.59	73.4
	4.34	0.13	97.0	4.48	0.69	84.6

CONCLUSION

αFe_2O_3NPs as adsorbent material was successfully synthesized and characterized. Its effectiveness for adsorbing heavy metal ions such as Pb^{2+} and $Cu^{2+}$was investigated using traditional Langmuir and Freundlich adsorption isotherms, showing a good fitting with Langmuir model. αFe_2O_3 NPs demonstrated high adsorption capacity for Pb^{2+} and lower affinity toward Cu^{2+} . The adsorbent was successfully used for removing heavy metal ions from waste sample solutions, highlighting its potential as a promising material in the field of separation science.

REFERENCES

[1] D. T.Sun, L.Peng, W. S.Reeder, S. M.Moosavi, D.Tiana, D. K.Britt, E.Oveisi, W. L. Queen,Rapid, selective heavy metal removal from water by a metal-Organic framework/polydopamine composite. ACS Cent. Sci. 4 (2018) 349−356.

[2] X.Lu, L.Wang, L. YLi., K.Lei, Huang, L.; Kang, D. Multivariate statistical analysis of heavy metals in street dust of Baoji, NW China. J. Hazard. Mater. 173 (2010) 744−749.

[3] S.Rajput, C. U.Pittman, D.Mohan, Magnetic magnetite (Fe_3O_4) nanoparticle synthesis and applications for lead (Pb^{2+}) and chromium (Cr^{6+}) removal from water. J. Colloid Interface Sci. 468 (2016) 334−346.

[4] Ö ztürk, D.; Sahan, T. Design and optimization of Cu (II) adsorption conditions from aqueous solutions by low-cost adsorbent.

[5] G.X. Zhao, L. Jiang, Y.D. He, J.X. Li, H.L. Dong, X.K. Wang, W.P. Hu, Sulfonated graphene for persistent aromatic pollutant management, Adv. Mater. 23 (2011) 3959–3963.

[6] Y.B. Sun, S.T. Yang, G.D. Sheng, Z.Q. Guo, X.L. Tan, J.Z. Xu, X.K. Wang, Comparison of U(VI) removal from contaminated groundwater by nanoporous alumina and non-nanoporous alumina, Sep. Purif. Technol. 83 (2011) 196–203.

[7] D.D. Shao, Z.Q. Jiang, X.K. Wang, J.X. Li, Y.D. Meng, Plasma induced grafting carboxymethyl cellulose on multiwalled carbon nanotubes for the removal of UO2 $^{2+}$ from aqueous solution, J. Phys. Chem. B 113 (2009) 860–864.

[8] H. Chen, J.X. Li, D.D. Shao, X.M. Ren, X.K. Wang, Poly(acrylic acid) grafted multiwall carbon nanotubes by plasma techniques for Co(II) removal from aqueous solution, Chem. Eng. J. 210 (2012) 475–481.

[9] J.X. Li, S.Y. Chen, G.D. Sheng, J. Hu, X.L. Tan, X.K. Wang, Effect of surfactants on Pb(II) adsorption from aqueous solutions using oxidized multiwall carbon nanotubes, Chem. Eng. J. 166 (2011) 551–558.

[10] V. Chandra, J. Park, Y. Chun, J.W. Lee, I.C. Hwang, K.S. Kim, Water-dispersible magnetite-reduced graphene oxide composites for arsenic removal, ACS Nano 4 (2010) 3979–3986.

[11] I. Akin, G. Arslan, A. Tor, M. Ersoz, Y. Cengeloglu, Arsenic(V) removal from underground water by magnetic nanoparticles synthesized from waste red mud, J. Hazard. Mater. 235 (2012) 62–68.

[12] H.Y. Koo, H.J. Lee, H.A. Go, Y.B. Lee, T.S. Bae, J.K. Kim, W.S. Choi, Graphenebased multifunctional iron oxide nanosheets with tunable properties, Chem. Eur. J. 17 (2011) 1214–1219.

[13] J.X. Li, Z.Q. Guo, S.W. Zhang, X.K. Wang, Enrich and seal radionuclides in magnetic agarose microspheres, Chem. Eng. J. 172 (2011) 892–897.

[14] X. Liu,Z.Ma,J.Xing,H.Liu,J.Magn.Magn.Mater.270 (2004)1–6.
[15] S. Suetal. S. Su, B. Chen, M. He, B. Hu , Z. Xiao,Talanta, 119 (2014)458–466.
[16]F. P.Fato, D.W. Li, L.J. Zhao, K.Qiu, Y.T. Long, ACS Omega 4 (2019) 7543–7549.
[18] L. Giraldo, A. Erto, J. C. Moreno-Piraján, Adsorption 19 (2013) 65−474.
[19] H.M.F. Freundlich, Over the adsorption in solution, Z. Phys. Chem., 57 (1906) 385–471.
[20] I. Langmuir, The adsorption of gases on plane surfaces of glass mica and platinum, J. Am. Chem. Soc., 40 (1918) 1361–1403.
[21] A.M. Donia, A.A. Atia, E.M.M. Moussa, A.M. El-Sherif, M.O. Abd El-Magied, Removal of uranium(VI) from aqueous solutions using glycidyl methacrylate chelating resins, Hydrometallurgy, 95 (2009) 183–189.
[22] P. Laiyaraja, A.K. Deb, K. Sivasubramanian, D. Ponraju, B. Venkatraman, Adsorption of uranium from aqueous solution by PAMAM dendron functionalized styrene divinyl benzene, J. Hazard. Mater., 250–251 (2013) 155–166.